JOURNAL OF PROPULSION AND POWER
Vol. 15, No. 2, March–April 1999

Comparative Analysis of the Windmilling Performance of Turbojet and Turbofan Engines

W. Braig,* H. Schulte,* and C. Riegler†
University of Stuttgart, 70569 Stuttgart, Germany

The windmilling performance of turbojet and turbofan (TF) engines is investigated numerically by means of a performance synthesis program. Different types of TF engines are taken into consideration, including mixed and unmixed exhaust configurations and configurations with and without a booster compressor on the low-pressure shaft. Furthermore, different design bypass ratios are investigated. The free windmilling performance is calculated for various ram pressure ratios, and, in addition, power input and offtake on the high-pressure shaft are considered. The calculated results indicate a rather strong dependency, not only on the design bypass ratio, but also on the engine type. For example, the internal drag and the maximum power offtake for a given ram pressure ratio differ considerably when comparing mixed and unmixed exhaust configurations. However, for the relight capability, the design bypass ratio is identified as the most important parameter. Nevertheless, the results of this investigation make evident that the rather widespread procedure to present the windmilling performance of engines dependent on ram pressure ratio and design bypass ratio is insufficient.

Nomenclature

A	= cross-sectional area
c	= velocity
g	= acceleration due to gravity
H	= flight altitude
M	= momentum
Ma	= Mach number
$\dot{m}$	= mass flow
n	= shaft speed
P	= power
p	= pressure
R	= specific gas constant
T	= temperature
V	= volume
μ	= bypass ratio
Π	= pressure ratio
Ψ, Ψ^*	= lighting parameter

Subscripts

BO	= booster compressor
D	= design point
FAN	= fan
H	= high-pressure shaft
L	= low-pressure shaft
max	= maximum
oa	= over all
off	= offtake
pz	= combustor primary zone
t	= total
0	= ambient
2	= inlet first compressor
3	= exit last compressor
4	= inlet first turbine
8	= nozzle throat
9	= nozzle exit
18	= bypass nozzle throat
24	= inlet high-pressure compressor

Received Oct. 13, 1997; revision received July 14, 1998; accepted for publication Aug. 11, 1998.

*Professor, Institut für Luftfahrtantriebe, Pfaffenwaldring 6.

†Professor, Institut für Luftfahrtantriebe; currently at German Aerospace Center, Institute for Propulsion Technology, Linder Hohe, 51147 Koln, Germany, stationed at MTU München, Engine System Simulation TPS2, Germany.

I. Introduction

DURING the normal operation of a turboengine installed in an aircraft, the combustor is supplied with fuel and the engine produces thrust. When the fuel flow to the combustor is cut off, the engine runs under so-called *windmilling conditions*, being driven only by the ram pressure ratio, and produces drag.

Regarding engines for conventional applications, windmilling is an extreme operating condition that usually is avoided during normal operation. During windmilling, the compressors and turbines, particularly, are working far away from their design points with rather poor efficiencies. Nevertheless, steady-state windmilling conditions may occur, for example, in the case of a flameout of one engine installed in a twin-jet. Therefore, the windmilling performance must be determined during the design and development of an engine. The most relevant data of windmilling performance are as follows: 1) the thermodynamic variables of state and the mass flow in the combustor regarding relight capability; 2) the shaft speeds and the maximum power that can be taken off the shafts to drive external devices such as hydraulic pumps, generators etc.; and 3) the drag the engine produces with regard to the flight performance of the aircraft.[1]

Regarding turboramjet propulsion systems for hypersonic applications, a transition from turbo to ram mode and a relight of the turboengine from windmilling is necessary, even during normal operation.[2] Therefore, compared with conventional applications for such a propulsion system, evaluation of the windmilling performance is even more important.

Because of the rather small variety of turbojet (TJ) engine configurations and design parameters, the windmilling performance of different TJ engines can be described by generally applicable correlations.[1,3] On the contrary, the variety of turbofan (TF) engine configurations and design parameters, particularly design bypass ratio, is much larger, resulting in a diverse windmilling performance.[1] Investigations dealing with the windmilling performance of particular TF engines[4,5] therefore cannot be applied to other configurations. A first investi-

gation of various TF engine types was presented in Ref. 6, showing the different windmilling performances caused by different design bypass ratios for mixed and unmixed exhaust configurations.

In this paper, a rather wide-ranging investigation is presented, dealing with the windmilling performance of TJ and TF engines. Corresponding to the wide range of engine types and design parameters under consideration, a theoretical approach is chosen, using a performance synthesis program.

II. General Aspects of Windmilling Performance

Starting with the TJ engine, the basic influence of the engine configuration on windmilling performance is discussed briefly and the governing parameters are introduced. A more detailed description of the fundamentals of windmilling performance of TJ engines is presented in Ref. 1.

A. Straight TJ Engine

There is no fuel flow and temperature rise across the combustor under windmilling conditions, and so the main parameter defining windmilling performance is the ram pressure ratio p_{t2}/p_0. Provided there is no power and air offtake, the nozzle total temperature T_{t8} is equal to the ram temperature T_{t2}. Because of the rather low turbomachinery efficiencies and the pressure losses in the flow ducts and in the combustor, the nozzle total pressure p_{t8} is usually far below the ram pressure p_{t2}. Correspondingly, the engine pressure ratio p_{t8}/p_{t2} is well below unity, resulting in a small nozzle pressure ratio p_{t8}/p_0. Consequently, the mass flow $\dot{m}_2$ is much lower than design and, as a result of $c_9 < c_0$, the engine produces drag.

Regarding additional power offtake for a given compressor pressure ratio, the turbine pressure ratio must be increased, resulting in falling pressure ratios p_{t8}/p_{t2} and p_{t8}/p_0. Hence, power offtake results in a smaller mass flow parameter for a given ram pressure ratio.

B. Unmixed Exhaust TF Engine

For configurations without a booster compressor on the low-pressure shaft, under windmilling operation, the power of the low-pressure turbine and, hence, of the fan is small. Therefore, the low-pressure shaft speed is given by the fan characteristics for low-power operation and for the flow passed through the fan. This results in a fan pressure ratio close to or slightly below unity and, hence, the pressure ratio for the bypass nozzle is close to the ram pressure ratio. The core flow can be assessed considering the core as a straight TJ engine with the low-pressure turbine representing the nozzle. As the passages of that turbine are small relative to the core nozzle, the core flow is rather small. For engines designed for a high bypass and high compression ratio, the large bypass nozzle throat area and the high bypass nozzle pressure ratio provide a large flow compared with core flow. This results in bypass ratios well above the design values and also in shaft speed ratios n_L/n_H higher than design, at least up to moderate ram pressure ratios.

A booster compressor on the low-pressure shaft prevents the fan speed accommodation for low-power operation described earlier, as the booster takes power from the low-pressure shaft to load the core, resulting in a lower shaft speed. Compared with the previously described configuration, the lower fan speed causes a lower bypass flow. Because of the core loading, the density at the core inlet and the pressure ratio across the core are increased. This leads to a higher core mass flow and a higher pressure and temperature in the combustor that are favorable for relight. However, these effects may be limited by the maximum acceptable booster pressure ratio requiring a booster exit bleed flow.

C. Mixed Exhaust TF Engine

For mixed exhaust configurations without a booster compressor on the low-pressure shaft, the driving pressure difference for the core from fan exit to mixing plane corresponds to the bypass duct pressure drop. The large bypass duct passages of high bypass ratio engines provide small pressure differences only. Therefore, in comparison with the unmixed exhaust engine, the mixed configuration is characterized by a higher pressure at the low-pressure turbine exit and, hence, by a lower core flow relative to bypass flow. This results in higher bypass ratios, higher shaft speed ratios n_L/n_H, and a lower combustor pressure and temperature that are unfavorable for relight.

With a booster compressor on the low-pressure shaft, energy is transferred from the bypass to the core flow, loading the core as described for the unmixed configuration. Compared with the mixed nonbooster version, the bypass ratio is lower and the combustor pressure and temperature are higher.

III. Engine Design

A. Engine Types and Thermodynamic Cycles

Corresponding to Sec. II, the numerical investigation is performed for a single-shaft TJ engine and for several twin-shaft TF engines, including 1) mixed and unmixed exhaust configurations and 2) TFs with and without the installation of a booster compressor on the low-pressure shaft. Furthermore, TFs with different bypass ratios are considered. The particular pressure ratio $p_{t3,D}/p_{t2,D}$ and temperature ratio $T_{t4,D}/T_{t2,D}$ are similar to those of realized engines with a corresponding bypass ratio.

Figure 1 shows the schematic views of all engines analyzed in this paper and the abbreviations used to address the engines in the following text.

The engine design calculations are carried through with the performance calculation program described in Ref. 2. The flight altitude H and the flight Mach number Ma_0 are chosen as typical values corresponding to the specific engine type. The following design parameters are chosen according to existing engines: 1) overall compressor pressure ratio $\Pi_{oa,D}$, 2) turbine inlet temperature $T_{t4,D}$, and 3) bypass ratio μ_D. In addition, for the TFs, the fan pressure ratio is adjusted for equal total pressure in the core and bypass flow at the mixer entry or at the entry of the core and bypass nozzle, respectively. For TFs with a booster compressor, the distribution of the core compressor pressure ratio on the booster and high-pressure compressor again is fixed following the data of existing engines, and in the same way, other data as, e.g., the efficiencies of the turbomachines, are fixed. The main design data are listed in Table 1.

B. Turbomachines

The aerodynamic design calculations for the turbomachines are carried through using midsection calculation procedures for compressors, fans, and turbines. The same design procedure and adequate technological parameters are used for the corresponding turbomachines of the different engines to provide results not affected by special design features of an individual engine type. Additionally, the turbomachines of the TF engine TF 2 are also used for the TF 4, because both engines realize the same thermodynamic cycle. This relation holds as well for the TF engines TF 3 and TF 5. Furthermore, for all TF engines with a bypass ratio of 4.7 (TF 2–TF 5), the same fan is used.

IV. Off Design Performance

A. Characteristics of Turbomachines

With the geometric data resulting from aerodynamic design calculations, the performance of the turbomachines is calculated over a wide range of operating conditions using midsection calculation procedures for compressors and turbines.

The characteristics are calculated based on the inlet conditions corresponding to the design point. The dependencies on variable Reynolds number and variable isentropic exponent are neglected.

Table 1 Engine types and main design parameters of the engines analyzed

	Engine types						
Engine	TJ	TF 1	TF 2	TF 3	TF 4	TF 5	TF 6
Mixed	——	Yes	Yes	Yes	No	No	No
Booster	——	No	Yes	No	Yes	No	Yes
Shafts	1	2	2	2	2	2	2
			Flight conditions				
H, km	11	0	11	11	11	11	11
Ma_0	0.9	0.0	0.9	0.9	0.9	0.9	0.9
			Design parameters				
$\Pi_{oa,D}$	10	25	32	32	32	32	40
$T_{t4,D}$, K	1400	1750	1500	1500	1500	1500	1500
μ_D	——	0.5	4.7	4.7	4.7	4.7	9.0
$\Pi_{FAN,D}$	——	4.324	1.689	1.689	1.683	1.683	1.465
$\Pi_{BO,D}$	——	——	1.263	——	1.263	——	2.2

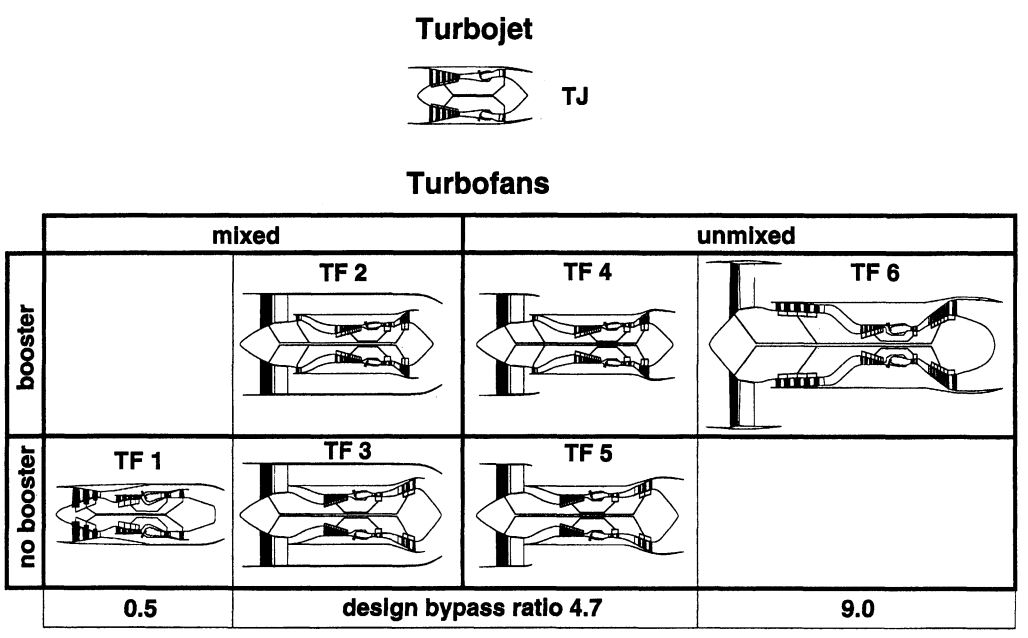

Fig. 1 Analyzed engines defined by engine type and design bypass ratio.

At the fan exit, equal total pressure and temperature is assumed in the core and bypass flow. The influence of the bypass ratio on the fan characteristics is also neglected.

B. Engine Performance

The windmilling performance of the engines analyzed is calculated using the performance synthesis program described in Ref. 2. In the calculation procedure the performance of turbomachines is included, applying their characteristics (see Sec. IV.A). The computer code is modular structured, allowing the numerical investigation of different types of engines with the same calculation procedure without a code change.

Except for efficiencies in turbomachines and pressure losses in flow ducts and combustors, no additional losses are taken into account here. Particularly, the losses caused by oil viscosity, etc., are neglected.

Because of the high shaft speed ratio n_L/n_H during windmilling, compared with the design value, the booster is likely to run out off surge margin, as already mentioned in Sec. II.B. Therefore, to keep the booster out of surge, bleed air is taken from the core flow into the bypass flow at the booster exit. Variable stator blades to improve high-pressure compressor efficiency are not considered.

The performance of the engines analyzed is calculated in free windmilling operation and with power input or power offtake on the high-pressure shaft, respectively. The ram pressure ratio as an independent parameter is varied between 1.0 and the value corresponding to a flight Mach number, which is typical for the engine type considered. The power taken off the high-pressure shaft is varied up to the maximum value that can be reached for a given ram pressure ratio.

V. Results

A. TJ Engine in Free Windmilling Operation

The windmilling performance of straight TJ engines is analyzed and discussed in several published papers.[1,3] Therefore, the results for the TJ are not discussed in detail in this paper. To assess the quality and reliability of the calculated data, engine mass flow parameters calculated for the TJ are plotted in Fig. 2 vs flight Mach number in a diagram that is drawn from Ref. 3. The data in Ref. 3 are obtained by means of experimental investigation for several TJ engines with different design parameters. The curve for the TJ analyzed in this paper fits with the data drawn from Ref. 3 and, hence, indicates the reliability of the calculated results.

B. Power Offtake or Input

As windmilling performance is sensitive to power offtake this is considered in more detail, using TF 1 as an example.

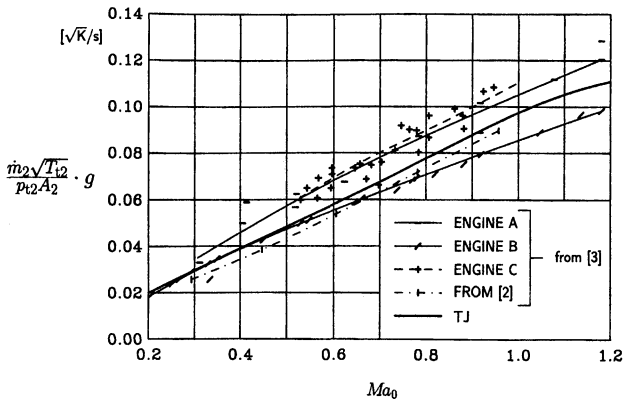

Fig. 2 Engine mass flow parameters for TJ and for several TJ engines analyzed in Ref. 3.

In Fig. 3 the engine mass flow parameter for the TF 1 is plotted vs ram pressure ratio for free windmilling conditions as well as for power offtake and input, the latter corresponding to starter-assisted windmilling. Here as an independent parameter, the ram pressure ratio is used instead of the flight Mach number, because by doing so, the plotted curves are valid for different pressure losses in the engine intake.

For the explanation of Fig. 3, the effect of offtake momentum at a constant ram pressure ratio is considered (Fig. 4). An increase of momentum results in a decrease of the mass flow parameter and high-pressure shaft speed. As the power offtake is given by the product of momentum and shaft speed, an increase of power depends on whether or not the increase of momentum prevails over the decrease of shaft speed. Starting with a momentum of zero (free windmilling), the relative increase of momentum dM_{off}/M_{off} exceeds the relative decrease of shaft speed dn_H/n_H and, hence, the power offtake increases.

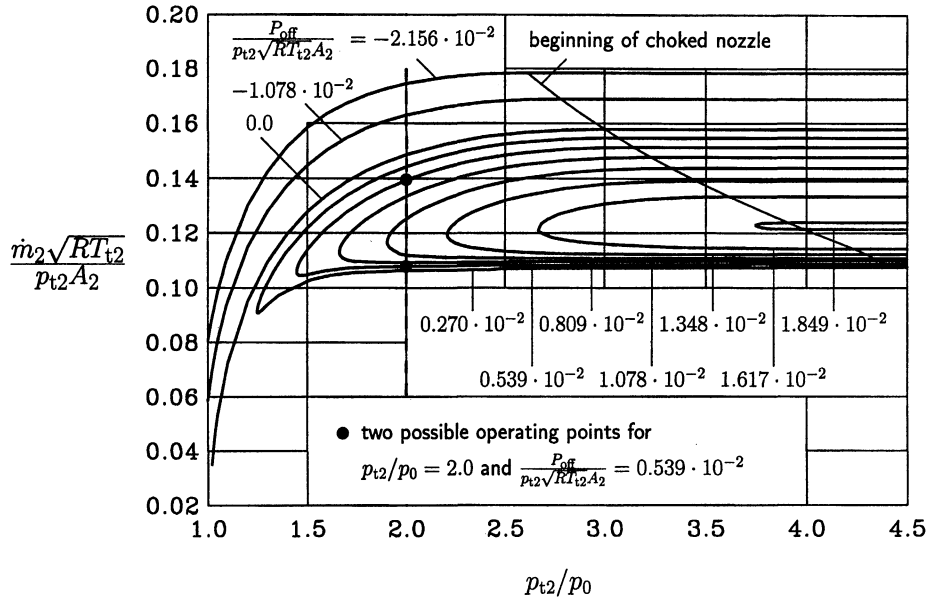

Fig. 3 Engine mass flow parameter for TF 1 vs ram pressure ratio with power offtake as a parameter.

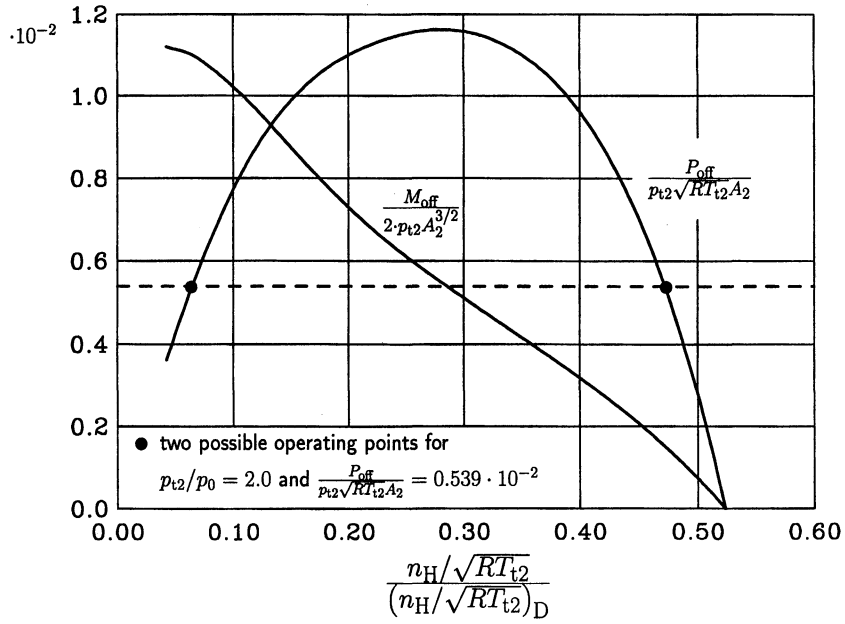

Fig. 4 Momentum and power offtake for TF 1 vs high-pressure shaft speed for $p_{t2}/p_0 = 2.0$.

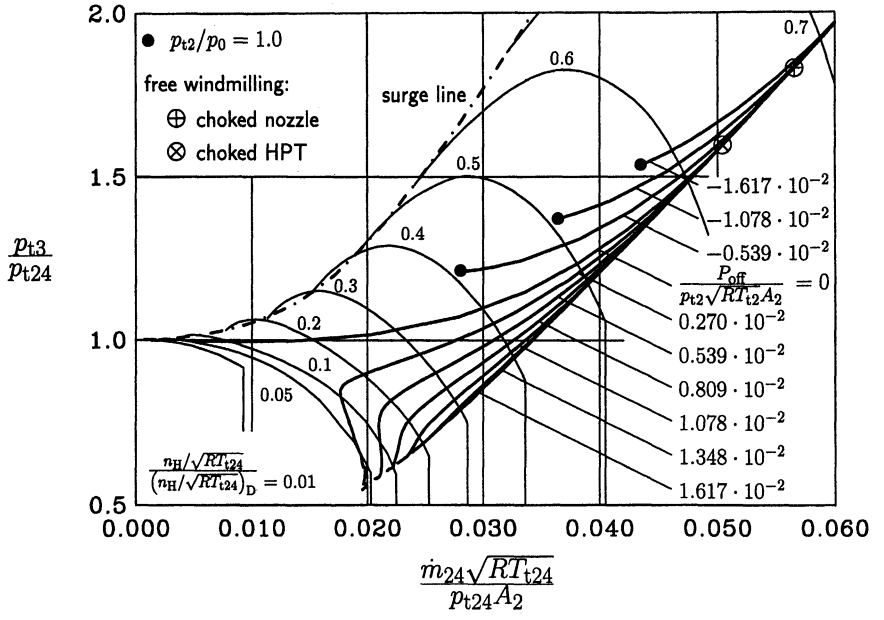

Fig. 5 Windmilling performance of TF 1 presented in the high-pressure compressor map.

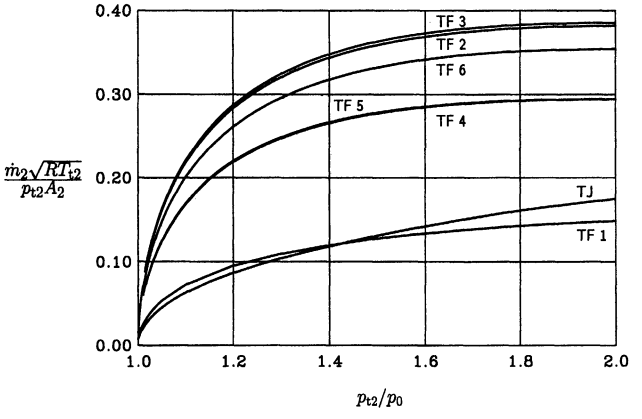

Fig. 6 Engine mass flow parameter, free windmilling.

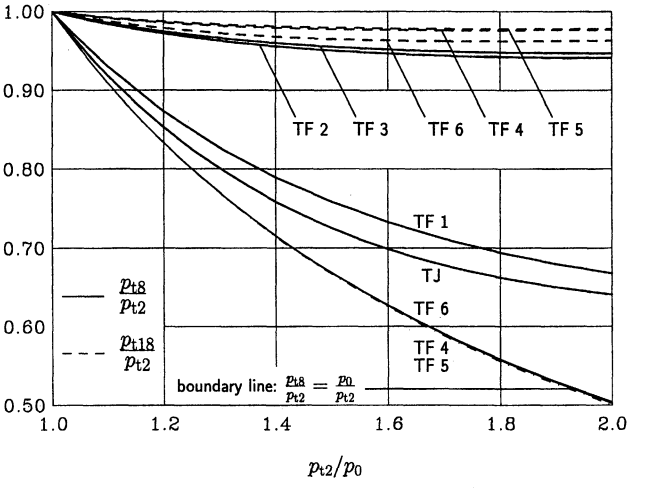

Fig. 7 Engine pressure ratio and fan pressure ratio, free windmilling.

For equal relative momentum increase and relative shaft speed decrease, the power offtake vs the high-pressure shaft speed shows a maximum value (Fig. 4). But for high momentum at a further momentum increase, the shaft speed decrease is dominating and, therefore, the power offtake decreases again. Finally, because of the limited momentum for the high-pressure shaft speed approaching zero, the corresponding power offtake also approaches zero. The shaft speed, where the maximum occurs, and the maximum power offtake are dependent on the development of momentum vs shaft speed and, hence, on the turbomachine efficiencies. Consequently, for a given power offtake and given ram pressure ratio, there exists two operating points; this can also be seen from Fig. 3.

The maximum power offtake increases with ram pressure ratio up to a chocked nozzle. Vice versa for a given demand of power offtake, a minimum value of ram pressure ratio is necessary.

For a given ram pressure ratio, with increasing offtake momentum, the turbomachine efficiencies become poorer; the engine pressure ratio and, hence, the nozzle pressure ratio are lower, too. Therefore, as shown in Fig. 3, the choked nozzle boundary line moves toward higher ram pressure ratios with increasing offtake momentum.

In Fig. 5, the windmilling performance of the TF 1 is presented in the high-pressure compressor map. For power input, the calculations were performed down to a minimum ram pressure ratio of 1.0, resulting in an ending of the lines of constant power input rather far away from the surge line. For a given power offtake or input, respectively, higher ram pressure ratios choke the high-pressure turbine (HPT) before the nozzle. This is obvious from Fig. 5 because the lines for different power offtake or input, respectively, are running together in a single curve, describing the throttling characteristic of the choked HPT. The end of the lines is reached for a choked nozzle because then a further increase of ram pressure ratio no longer affects the flow upstream of the nozzle throat. On the free windmilling operating line, the operating points for the beginning of choked HPT and choked nozzle are marked in Fig. 5.

C. Comparison of Different Configurations

On the basis of the well-known windmilling performance of TJ engines and of the relations valid for power offtake discussed in Sec. V.B, the windmilling performance data of all engines analyzed in this paper are compared. Figures 6–11 show the free windmilling performance data dependent on ram pressure ratio. Figure 12 shows the maximum power offtake vs ram pressure ratio. All diagrams are presented with similarity parameters to ensure comparability and applicability to different flight conditions. The parameters for mass flow, internal drag, and power offtake are related to A_2 to take the

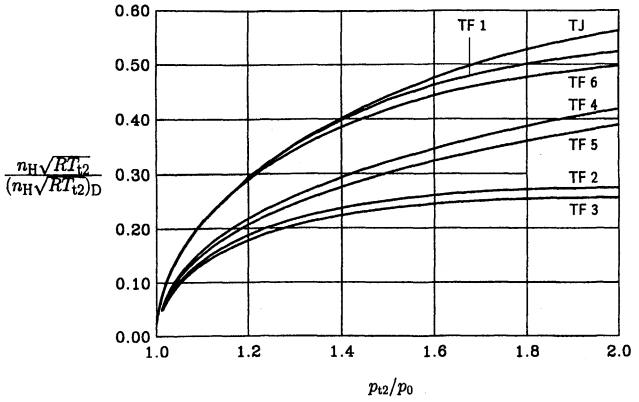

Fig. 8 High-pressure shaft speed relative to design, free windmilling.

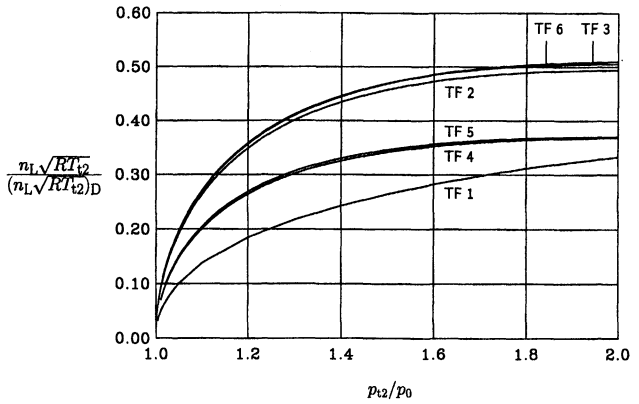

Fig. 9 Low-pressure shaft speed relative to design, free windmilling.

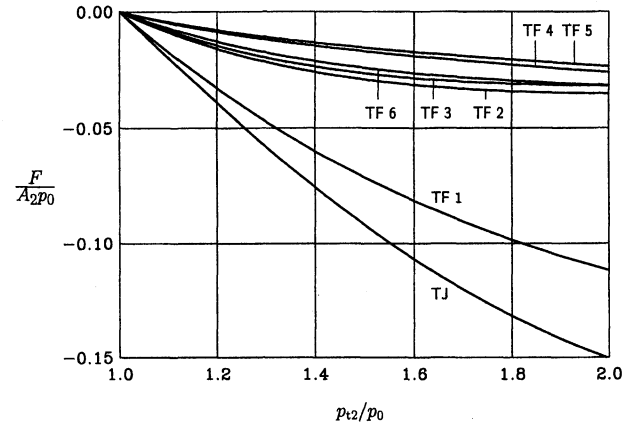

Fig. 10 Internal drag, free windmilling.

engine size into consideration. To estimate relight capability, Ψ from Ref. 7,

$$\Psi = (0.67 \cdot \dot{m}_3)/(p_{t3}^{1.3} \cdot V_{pz} \cdot 10^{T_{t3}/700}) \quad (1)$$

is used in Fig. 11 in a nondimensional form:

$$\Psi^* = \Psi/[A_2/(V_{pz} \cdot p_{t2}^{0.3} \cdot \sqrt{RT_{t2}})] \quad (2)$$

Low values of Ψ^* correspond to good relight capability. Ψ^* is applicable to different A_2 and p_{t2}. However, the plotted curves are valid for T_{t2} = 288.15 K only, because variable T_{t2} is not covered with the parameter Ψ^*, caused by the influence of $T_{t3}/700$. Notice that Ψ^* shows the important influence of V_{pz} on relight capability.

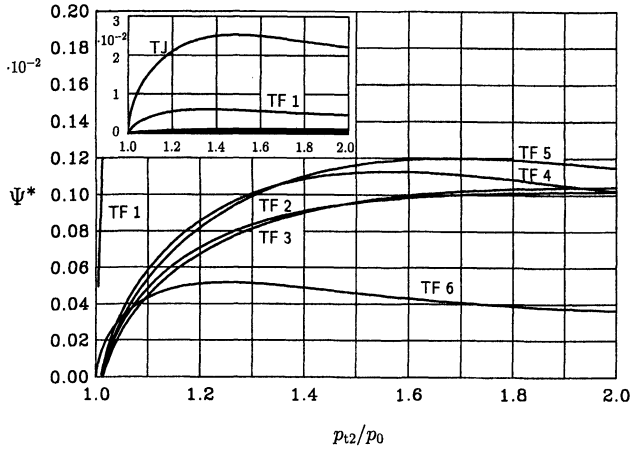

Fig. 11 Nondimensional lighting parameter for T_{t2} = 288.15 K, free windmilling.

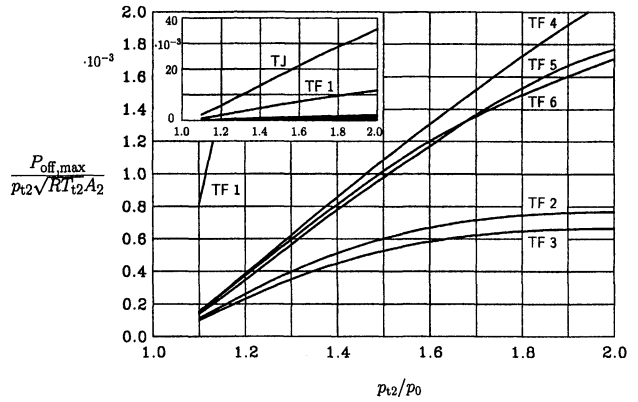

Fig. 12 Maximum power offtake.

1. TF Engines TF 2–TF 5

The TF engines TF 2–TF 5 have equal design parameters $p_{t3,D}/p_{t2,D}$, $T_{t4,D}/T_{t2,D}$, and μ_D and use the same fan. TF 5 has an unmixed exhaust configuration and no booster and, hence, shows small thermodynamic coupling between core flow and bypass flow. Therefore, in the following, TF 5 is used as a reference. For engines TF 2–TF 5 in free windmilling operation, the fan works as a turbine, putting power into the low-pressure shaft. This behavior is typical for high design bypass ratios.[6]

TF 5. As already depicted in Sec. II.B for TF 5, the fan pressure ratio is slightly below unity (Fig. 7), resulting in a bypass nozzle pressure ratio close to the ram pressure ratio. As the passages in the core engine are rather small and the losses in the turbomachinery are fairly high, the engine pressure ratio p_{t8}/p_{t2} and, hence, the core nozzle pressure ratio, are also rather small. This can be seen in Fig. 7, where the curve for TF 5 is located next to the boundary line with $p_{t8} = p_0$. This results in a core mass flow relative to engine mass flow far beyond the design value. In accordance with the mass flows, the shaft speeds relative to design are higher on the low-pressure shaft compared with the high-pressure shaft, at least for small values of ram pressure ratio, as can be seen from Figs. 8 and 9. Because of the comparatively low core flow and the high bypass nozzle pressure ratio, the internal drag of TF 5 is small compared with the TJ (Fig. 10).

As far as the relight capability is concerned, the TF 5 engine shows much better values of Ψ^* than the TJ, as can be seen from Fig. 11. For an explanation, the nondimensional lighting parameter is rewritten as

$$\Psi^* = 0.67 \cdot \frac{\dot{m}_2\sqrt{RT_{t2}}}{p_{t2}A_2} \cdot \frac{\dot{m}_3}{\dot{m}_2} \cdot \left(\frac{p_{t2}}{p_{t3}}\right)^{1.3} \cdot \frac{1}{10^{T_{t3}/700}} \quad (3)$$

The dominant parameter is the core mass flow relative to engine mass flow $\dot{m}_3/\dot{m}_2$, which is 1.0 for the TJ, and reaches values of about 0.02 for TF 5.

Corresponding to the low high-pressure shaft speed and core mass flow, the maximum power offtake is rather small as well (Fig. 12).

TF 4 Compared with TF 5. With a booster on the low-pressure shaft of TF 4, power is transferred from the bypass flow to the core flow, resulting in lower fan speed, lower fan pressure ratio, slightly lower engine mass flow, and higher internal drag compared with TF 5. On the contrary, the core is loaded by the additional booster pressure ratio. The core pressure ratio p_{t8}/p_{t24} is smaller, and the core flow relative to engine mass flow is larger. Consistent with the higher p_{t24} and the higher core mass flow for equal ram pressure ratio, the high-pressure shaft speed and the total pressure at the combustor inlet are higher compared with TF 5. For a sufficiently high ram pressure ratio, this results in lower Ψ^* and better relight capability compared with TF 5 (Fig. 11). The maximum power offtake is also higher because of the higher mass flow and pressure in the core. Because of the mechanical coupling with the fan and the thermodynamical coupling with the high-pressure compressor, in windmilling the booster is running with comparatively high shaft speed and comparatively low mass flow, which necessitates a booster exit bleed flow to prevent booster surge. Therefore, and also as a result of the comparatively low booster design pressure ratio of TF 4, the differences between TF 4 and TF 5 in windmilling performance are moderate. As seen in Fig. 6, barely any difference in mass flow parameter is evident.

TF 3 Compared with TF 5. For the mixed exhaust configuration TF 3, the pressure at the low-pressure turbine exit is given by the fan pressure ratio and the bypass duct pressure loss, which is comparatively small because of the large bypass duct passages of TF 3. This results in a rather high pressure at the low-pressure turbine exit, high values of p_{t8}/p_{t2} and p_{t8}/p_{t24}, and hence, a very low core mass flow relative to engine mass flow and low high-pressure shaft speed compared with TF 5. For TF 3, the lower core mass flow relative to the engine mass flow results in lower Ψ^* and better relight capability compared with TF 5 in the entire range of ram pressure ratios shown in Fig. 11. In accordance with the low core mass flow, the maximum power offtake is much lower than for TF 5. On the contrary, the large bypass duct passages provide large bypass mass flow, high fan speed, and low fan pressure ratio. The internal drag is higher compared with TF 5 as a result of the higher engine mass flow and the low nozzle pressure ratio, the latter compared with the bypass nozzle pressure ratio of TF 5. For the mixed exhaust configuration TF 3, the values of p_{t8}/p_{t2} are slightly below unity choking the nozzle for ram pressure ratios of approximately 2.0 (Figs. 6–11).

TF 2 Compared with TF 3. With a booster on the low-pressure shaft of TF 2, power is transferred from the bypass flow to the core flow, loading the core and reducing the bypass flow. This results in lower fan speed, lower fan pressure ratio, and lower pressure at the low-pressure turbine exit. The core pressure ratio p_{t8}/p_{t24} becomes smaller, giving a higher core mass flow relative to the engine mass flow. The differences in windmilling performance between TF 2 and TF 3 are close to those between TF 4 and TF 5 and, therefore, are not discussed further.

2. *TF Engines TF 6 and TF 4*

TF engines TF 4 and TF 6 are both unmixed exhaust configurations with a booster on the low-pressure shaft. The main difference is the design bypass ratio. The higher design bypass ratio of TF 6 gives an engine design with more power on the low-pressure shaft relative to the high-pressure shaft, a smaller fan design pressure ratio, and a significantly higher booster design pressure ratio (Table 1). As a result of the moderate fan design pressure ratio, the bypass nozzle passage of the TF 6 is rather large relative to the mass flow.

In free windmilling operation resulting from the large bypass nozzle passage, the mass flow of TF 6 is large compared with TF 4, despite the slightly smaller fan pressure ratio that is still close to unity. The large power output of the fan driving the low-pressure shaft accordingly gives high low-pressure shaft speed relative to design compared with TF 4. In agreement with the higher mass flow and the lower bypass nozzle pressure ratio, the internal drag is higher for TF 6 than for TF 4. As mentioned earlier for configurations with a booster compressor, the booster is stabilized in windmilling by booster exit bleed, so that the booster runs with a given surge margin. Because the booster of TF 6 has a design pressure ratio larger than the TF 4 booster and because the low-pressure shaft speed relative to design is higher for the TF 6, the booster pressure ratio in windmilling operation is much higher for TF 6 than for TF 4. Therefore, the core is loaded much more and the high-pressure shaft speed relative to design is higher compared with TF 4. In addition, the total pressure at combustor inlet p_{t3} is much higher for TF 6, resulting in a better relight capability (Fig. 11). The maximum power offtake related to A_2 is lower for TF 6 compared with TF 4, because with a higher design bypass ratio, the high-pressure shaft power relative to the low-pressure shaft power is lower. However, this tendency is partly compensated by the high windmilling pressure ratio of the booster of TF 6, loading the core and, hence, shifting the curve for TF 6 to higher values in Fig. 12.

3. *TF Engines TF 1 and TF 3*

TF engines TF 1 and TF 3 are both mixed-exhaust configurations without a booster. The main differences are caused by the design bypass ratio. The lower design bypass ratio of TF 1 gives an engine design with more power on the high-pressure shaft relative to the low-pressure shaft and a much larger fan design pressure ratio (Table 1). As a result of the large fan design pressure ratio, the bypass duct passages of TF 1 are rather small relative to the mass flow when compared with TF 3.

In windmilling operations, as a result of the rather small bypass duct passages of TF 1, the incoming air cannot bypass the core engine with its large aerodynamic losses, as is possible with larger μ_D. And so, in TF 1, both the core engine and the bypass duct produce rather large pressure losses, resulting in small values of p_{t8}/p_{t2} and, hence, in a small engine mass flow compared with TF 3. Despite the low engine mass flow, the internal drag is very high compared with TF 3 because of the small values of p_{t8}/p_{t2}. Consistent with the rather high core mass flow, the high-pressure shaft speed relative to design is higher compared with TF 3, resulting in higher p_{t3}/p_{t2}. Because of the high core mass flow relative to engine mass flow, according to Eq. (3), the values of Ψ^* are higher and, hence, relight capability is worse for TF 1 compared with TF 3. The maximum power offtake related to A_2 is also higher, because of the larger power of the high-pressure shaft relative to the low-pressure shaft.

VI. Conclusions

The steady-state windmilling performance of seven different engines was investigated numerically by means of a performance synthesis program. Apart from a straight TJ engine, six TF engines were studied, including three different design bypass ratios, mixed and unmixed exhaust configurations, and engines with and without booster compressor on the low-pressure shaft.

The calculated results show a rather strong dependency, not only on the design bypass ratio, but also on the engine type. Whereas the relight capability is mainly dependent on design bypass ratio, the low- and high-pressure shaft speeds and the internal drag and maximum power offtake are in addition strongly affected by engine configuration. Therefore, the rather widespread procedure to present the windmilling performance

of engines dependent on ram pressure ratio and design bypass ratio only is insufficient to characterize engine behavior.

The results produced with a performance synthesis program are plausible and were compared as far as possible with the published data. Hence, providing a proper modeling of the turbomachinery over a sufficiently wide range, a numerical investigation with a performance synthesis program can be used to understand the relations and to predict the parameters even in such extreme operating conditions as windmilling.

Nevertheless, for a better understanding and a confirmation of the numerical results experimental investigation concerning the far-off design performance of turbomachines, particularly fans followed by a flow diverter, and the windmilling performance, particularly of turbofan engines, would be very useful.

Acknowledgments

The work leading to the results described in this paper was partly supported by the Deutsche Forschungsgemeinschaft within the frame of the Collaborative Research Center (Sonderforschungsbereich) SFB 259.

References

[1]Walsh, P. P., and Fletcher, P., "Windmilling," *Gas Turbine Performance*, Blackwell Science, Oxford, England, UK, 1998, pp. 501–518.

[2]Therkorn, D., "Fortschrittliches Leistungs-Berechnungsverfahren für luftatmende Turbotriebwerke," Ph.D. Dissertation, Univ. of Stuttgart, Inst. für Luftfahrtantriebe, Stuttgart, Germany, Jan. 1992.

[3]Shou, Z. Q., "Calculation of Windmilling Characteristics of Turbojet Engines," *Journal of Engineering for Power*, Vol. 103, Jan. 1981, pp. 1–12; also American Society of Mechanical Engineers, Paper 80-GT-50, March 1980.

[4]Morita, M., Sasaki, M., and Torisaki, T., "Restart Characteristic of Turbofan Engines," International Society for Air Breathing Engines, Paper 89-7127, 1989.

[5]Choi, M., Kang, I., Lim, J., and Hong, Y., "Analysis of Windmilling Characteristics for a Twin-Spool Turbofan Engine," American Society of Mechanical Engineers, Paper 97-AA-113, Sept. 1997.

[6]Anderson, B. A., Messih, D., and Plybon, R. C., "Engine-Out Performance Characteristics," International Society for Air Breathing Engines, Paper 97-7216, Sept. 1997.

[7]Hagen, H., *Fluggasturbinen und ihre Leistungen*, G. Braun, Karlsruhe, Germany, 1982.